Journal of the International Neuropsychological Society (2007), **13**, 1–9.

DOI: 10.1017/S1355617707070646

CRITICAL REVIEW

Measurement of cerebral perfusion with arterial spin labeling: Part 1. Methods

THOMAS T. LIU[1] AND GREGORY G. BROWN[2,3]

[1]Department of Radiology, University of California San Diego, San Diego, California
[2]Psychology Service, VA San Diego Healthcare System, San Diego, California
[3]Department of Psychiatry, University of California San Diego, San Diego, California

(RECEIVED March 30, 2006; FINAL REVISION November 15, 2006; ACCEPTED November 16, 2006)

Abstract

Arterial spin labeling (ASL) is a magnetic resonance imaging (MRI) method that provides a highly repeatable quantitative measure of cerebral blood flow (CBF). As compared to the more commonly used blood oxygenation level dependent (BOLD) contrast-based methods, ASL techniques measure a more biologically specific correlate of neural activity, with the potential for more accurate estimation of the location and magnitude of neural function. Recent advances in acquisition and analysis methods have improved the somewhat limited sensitivity of ASL to perfusion changes associated with neural activity. In addition, ASL perfusion measures are insensitive to the low-frequency fluctuations commonly observed in BOLD experiments and can make use of imaging sequences that are less sensitive than BOLD contrast to signal loss caused by magnetic susceptibility effects. ASL measures of perfusion can aid in the interpretation of the BOLD signal change and, when combined with BOLD, can measure the change in oxygen utilization accompanying changes in behavioral state. Whether used alone to probe neural activity or in combination with BOLD techniques, ASL methods are contributing to the field's understanding of healthy and disordered brain function. (*JINS*, 2007, *13*, 1–9.)

Keywords: fMRI; Cerebrovascular circulation, Cerebral cortex, Brain, Regional blood flow, Microcirculation

INTRODUCTION

In healthy individuals, alterations in neural activity lead to changes in local cerebral blood flow (CBF). Since the work of Roy and Sherrington (Roy & Sherrington, 1890) CBF has been used as a marker of neural activity in cognitive and clinical neuroscience studies. Moreover, CBF can be combined with physiological parameters to reveal the complex neurobiology of healthy and disordered brain function. Typically radioactive tracers have been used to measure CBF. Because CBF measurement with radiotracers requires a specialized imaging unit, CBF is usually measured only in chronic medical disorders where patients are stable enough to be transported (Wintermark et al., 2005). To minimize overexposure to radiation and to prevent the radioactive tracer from the previous scan from affecting the subsequent scan, repeated CBF studies using radiotracers must include delays from a few minutes to an hour (Wintermark et al., 2005). Such delays reduce the usefulness of radiotracer CBF techniques as measures of short-term CBF dynamics. The delays also limit the usefulness of radioactive CBF measures in studies of practice effects, brain rehabilitation, and cognitive retraining. Recent developments in magnetic resonance imaging (MRI) have made possible the non-invasive measurement of regional CBF. These methods are highly repeatable and can produce images at moderately high spatial resolution. When MR perfusion and blood oxygenation level dependent (BOLD) contrast images are acquired in the same behavioral activation experiment, the change in metabolic rate of oxygen utilization can be inferred (Davis et al., 1998). These perfusion MRI methods, which rely on the traditional tracer-kinetic model, are discussed later.

Correspondence and reprint requests to: Thomas T. Liu, Ph.D., Center for Functional Magnetic Resonance Imaging, University of California San Diego, 9500 Gilman Drive, MC 0677, La Jolla, CA, 92037-0677. E-mail: ttliu@ucsd.edu

Background Principles

Cerebral blood flow

Cerebral blood flow is a measure of the volume of blood passing through a point in the brain circulation per unit time (Guyton, 1977). Cerebral perfusion is the delivery of blood to the capillary bed (Warner et al., 1987). The methods discussed later are based on perfusion models of CBF and have not been developed to measure venous flow. The standard unit of measurement for CBF is (milliliters of blood)/(100 grams of tissue)/(minute), and a typical value in human gray matter is roughly 60 mL/(100 g)/minute (Buxton, 2002). Assuming an average brain tissue density of 1 g/mL, the average CBF may be approximated as 60 mL/(100 mL)/(60 s) = 0.01 s^{-1}. Note that this last expression for CBF means that within a 1 second period approximately 1% of the total tissue volume consists of freshly delivered blood.

Measurement of cerebral blood flow with tracers

Methods for measuring CBF in humans include single photon emission computed tomography (SPECT), positron emission tomography (PET), MRI with contrast agents such as gadolinium, and arterial spin labeling MRI. These methods are all based on the measurement of the concentration of a tracer that is delivered to and cleared from the tissue by blood flow. Investigators often use the Meier and Zierler model to infer blood flow, F, from the arterial $C_A(t)$ and tissue concentration $C_T(t)$ of the tracer expressed as a function of time, t (Meier & Zierler, 1954). At any point in time t, the tissue concentration $C_T(t)$ of the tracer is a function of both the delivery and clearance of the tracer for a volume of interest (VOI). As a function of time, the delivery of the tracer depends on the product $F \cdot C_A(t)$ of the blood flow and the arterial concentration. To represent clearance of the tracer, a residue function $r(t)$ is used to indicate the fraction of the tracer that entered the VOI at time $t = 0$ and still remains at time t (Calamante et al., 1999). As described in Buxton (2002), the tissue concentration can be written as the product $C_T(t) = F \cdot A_{eff}$, where the term A_{eff} depends on the arterial concentration and residue function. If the arterial concentration of the tracer and the distribution of clearance rates are assumed to be the same in all brain regions, then A_{eff} will be constant across the brain, and maps of local variations in tissue concentration are quantitative maps of CBF variation scaled by A_{eff} (Buxton et al., 1998a).

Arterial Spin Labeling

General principles

In arterial spin labeling MRI, the tracer is a magnetic label applied to the water molecules of flowing blood. Typically the magnetic label is produced by saturating or inverting the longitudinal (Z-axis) component of the MR signal. Once in the capillaries, the tagged water passes into brain tissue, where it alters the local tissue's longitudinal magnetization (Aguirre et al., 2005). In the case of a saturation tag, blood flowing into an imaging slice reduces the T_1-weighted signal compared with a control image where blood is fully relaxed. Inversion tagging also reduces the signal in the imaging slice, but at twice the efficiency of saturation tagging. The greater the flow into the imaging slice, the greater the signal changes in the tagged condition compared with the control condition. Thus, most arterial spin labeling methods measure CBF by taking the difference of two sets of images: *tag images*, in which the longitudinal magnetization of arterial blood is inverted or saturated, and *control images* in which the magnetization of arterial blood is fully relaxed.

The two basic steps involved in ASL CBF methods are shown in Figure 1. First, arterial blood flowing toward the region of interest (ROI) is tagged by magnetic inversion or saturation (Fig. 1). This tagged blood flows into the imaging slices or volume and also relaxes toward equilibrium with the longitudinal relaxation time constant, T_1, of blood

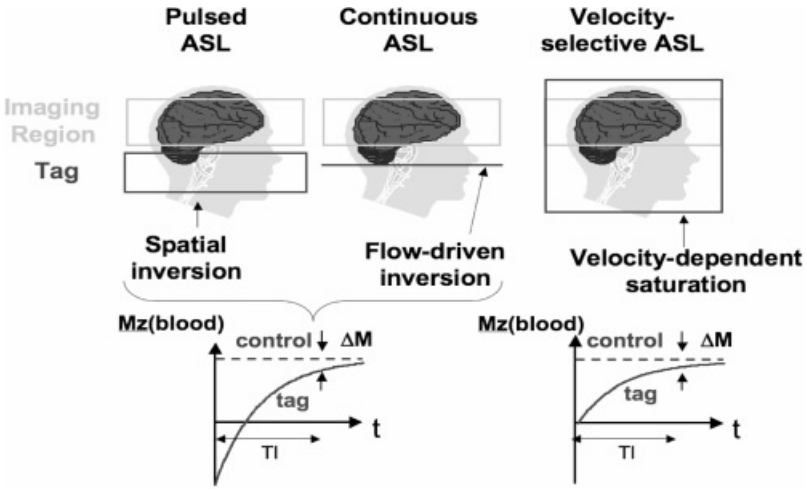

Fig. 1. Pulsed, continuous, and velocity-selective ASL methods use various techniques to either invert or saturate the magnetization of arterial blood. The difference ΔM between control and tag images is proportional to CBF.

(see solid curves in the bottom half of Fig. 1). Second, after a delay *TI* (known as the inversion time) to allow for inflow of tagged blood, an image is acquired in the slice(s) or volume of interest. This image is referred to as the *tag image*.

In a typical ASL experiment, about one second is allowed for the delivery of blood, corresponding to 1 mL of blood delivered to 100 mL of tissue (See above). As a result, the overall magnetic resonance (MR) signal caused by the delivered blood is only about 1% of the total signal due to the tissue. This small percentage contributes to the low intrinsic signal-to-noise ratio (SNR) of ASL methods.

In order to remove the contribution of the static tissue to the tag image, a *control image* of the same slice is acquired in which inflowing blood is not tagged. The magnetization of this control image is shown by the dashed lines in the bottom half of Figure 1. Taking the difference of the control and tag images yields an image $\Delta M = M_{control} - M_{tag}$ that is proportional to CBF. This is shown as the difference of the dashed and solid lines in Figure 1. Tag and control images are typically acquired in a temporally interleaved fashion, and the running difference of the control and tag images is used to form a perfusion time series (see Fig. 2 and section on Data Processing Choices).

We can treat the magnetization difference ΔM as the concentration of a tracer that is delivered by flow. The amount of magnetization difference present at time *t* will depend on the delivery of magnetization by arterial flow and the clearance of the magnetization by venous outflow and longitudinal relaxation (Buxton et al., 1998a). A common alternative framework to understand MR methods of CBF measurement is to consider the impact of flowing spins on the Bloch equations, the standard equations describing longitudinal and transverse relaxation (Calamante et al., 1999; Detre et al., 1992). These equations focus on the impact of flow on the longitudinal component of the tissue magnetization. Detre et al. (1992) and Calamante et al. (1999) should be consulted for greater detail. Buxton and colleagues discuss how the tracer kinetic model relates to the Bloch equation model (Buxton et al., 1998a).

Arterial spin labeling methods

There are currently three classes of ASL methods, as summarized in Figure 1. The methods vary according to the dependence of the magnetic labeling process on the location and velocity of the flowing blood.

Pulsed ASL (PASL)—tagging based on location. In these techniques, short (5–20 ms) RF pulses are used to saturate or invert a slab of spins (both static and flowing), known as the tagging region, which is proximal to the imaging slice in the region of interest (Edelman et al., 1994). These techniques have the advantages of high inversion efficiency and little RF power use. Disadvantages are that they depend on the coverage and uniformity of the transmit RF field to determine the geometry of the applied tag. Pulsed ASL methods include EPISTAR (Edelman et al., 1994), FAIR (Kim & Tsekos, 1997; Kwong et al., 1995), PICORE (Wong et al., 1997), and other variants. These methods differ in the details of the implementation of the tag and control conditions, but give very similar perfusion results (Wong et al., 1997).

Continuous ASL (CASL)—tagging based on location and velocity. In continuous ASL, long (1–3s) RF pulses are used in conjunction with a constant gradient field to irradiate a narrow plane of spins with RF energy. The plane is chosen proximal to the region of interest so that inflowing arterial blood flows through the plane in a direction that is roughly normal to the plane. When the amplitude of the RF and gradient fields are properly adjusted, inflowing spins within a physiological range of velocities will be labeled based on a phenomenon termed flow-driven adiabatic inversion (Williams et al., 1992). Because the tag can be applied closer than pulsed ASL to the region of interest (on average), the continuous method can result in a higher overall tagging efficiency than pulsed techniques. However, continuous ASL technique requires a large amount of average RF power and can be limited by both system performance capabilities and FDA guidelines governing how much RF energy can be absorbed per unit mass, the specific absorption rate, at higher fields (Alsop, 2005). Limitations because of system performance have been for the most part addressed in a recently introduced form of CASL, dubbed pseudo-CASL, that uses repeated RF pulses instead of a continuous RF wave (Garcia et al., 2005). A detailed comparison of pulsed and continuous ASL techniques can be found in Wong et al. (1998b).

Velocity selective ASL (VS-ASL)—tagging based on velocity. In this technique, the tagging scheme selectively saturates flowing spins with no spatial selectivity (Wong et al., 2006). This is accomplished with an RF and gradient pulse train that effectively dephases the MR signal from protons that are flowing faster than a specified cut-off velocity while rephasing the signal from slower flowing protons. For a typical cut-off velocity of 1 cm/sec, the sequence dephases spins in arterioles that are approximately 50 microns or more in diameter. In principle, this scheme results in a small and uniform transit delay for the delivery of the tagged blood to the tissues of interest (see later regarding transit delays).

Data processing

In most ASL fMRI experiments, control and tag images are acquired in an interleaved fashion, as shown in Figure 2. A perfusion time series is then formed from the running subtraction of the control and tag images. An example of this process is shown in Figure 2, where the perfusion images are formed from the difference between each control image and the average of the two surrounding tag images or from the difference between the average of two surrounding control images and a tag image. The type of differencing shown

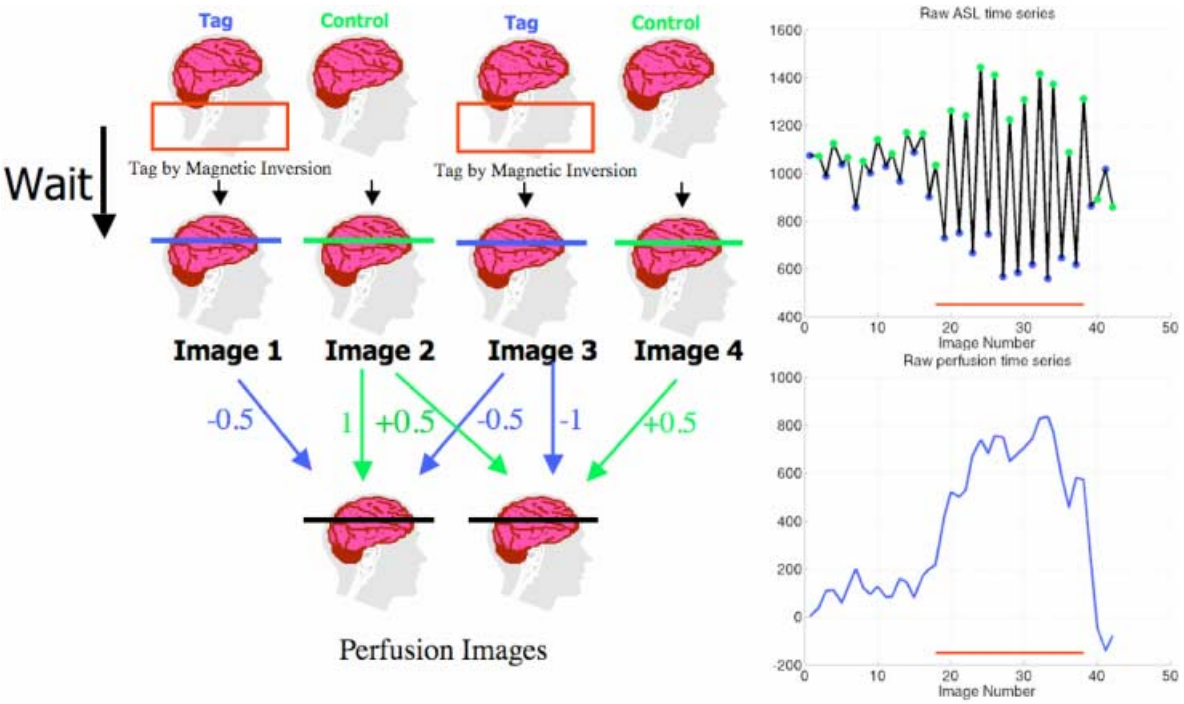

Fig. 2. Formation of a perfusion time series from the "surround subtraction" of control and tag images. An example time series of control (green) and tag (blue) signals is shown in the upper right-hand plot. The perfusion time series created by surround subtraction is shown in the lower right-hand plot. The solid red bars indicate the time of stimulus.

in Figure 2 is referred to as *surround subtraction*, and represents one specific approach to the *filtered subtraction* of control and tag images. If odd indexed images are control images and even indexed images are tagged, then surround subtraction over the image acquisition time series produces the perfusion weighted time series: $(\{y[1] - (y[0] + y[2])/2\}, \{(y[1] + y[3])/2 - y[2]\}, \ldots)$. Other common approaches are *pairwise subtraction* and *sinc subtraction*. A general analytic model is available to compare the performance of these three methods of subtraction (Liu & Wong, 2005). For fMRI experiments with block designs (e.g., long periods of on/off), surround and sinc subtraction tend to provide the best performance (Aguirre et al., 2002). In contrast, for randomized event-related designs, pair-wise subtraction can provide better performance (e.g. less filtering of the hemodynamic response function) (Liu & Wong, 2005). However, all filtered subtraction approaches lead to inevitable broadening of the hemodynamic response function. Unfiltered approaches based on general linear models of the ASL experiment can be used to eliminate this broadening (Liu et al., 2002), and can lead to improvements in statistical power (Mumford et al., 2006). Bayesian approaches to the analysis of ASL data also show promise for increasing the sensitivity of ASL measures (Woolrich et al., 2006).

As with BOLD fMRI experiments, cardiac and respiratory fluctuations are a major source of noise in ASL experiments, especially at higher field strengths. Because the inherent SNR of ASL methods is typically lower than that of BOLD fMRI, the need for methods to reduce physiological noise is especially pronounced. Retrospective image-based correction methods have been shown to significantly reduce physiological noise in ASL data (Restom et al., 2006). An example is shown in Figure 3.

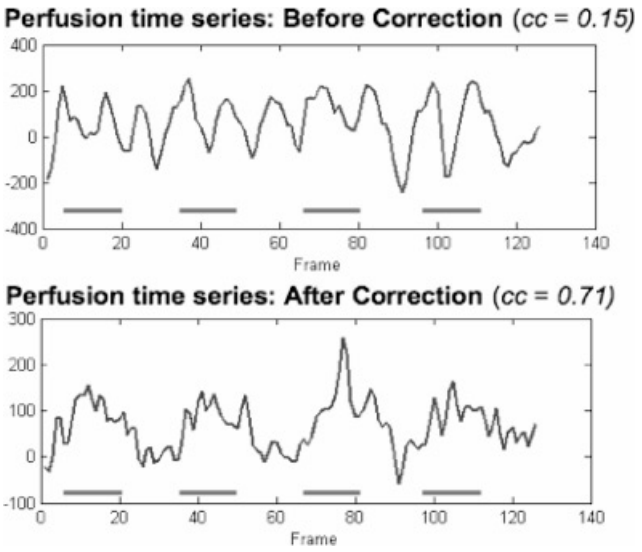

Fig. 3. Example of a perfusion time series before (top) and after (bottom) the application of physiological noise correction. The solid horizontal bars indicate the times when a stimulus was applied.

Simultaneous estimates of BOLD and CBF

ASL data for fMRI are often acquired with single-shot acquisition methods such as echo-planar imaging (EPI) or spiral readouts. In addition to their sensitivity to flow introduced by the tagging process, EPI or spiral images can also exhibit BOLD contrast. For example, with gradient echo readouts and sufficiently long echo times, the images exhibit a BOLD weighting. Dual echo acquisitions are particularly useful for simultaneous perfusion and BOLD imaging. Images acquired at a short echo time (e.g. 3 ms) can be used to form a perfusion time series with relatively little BOLD weighting, whereas images acquired at a later echo time (e.g. 30 ms) can be use to form the BOLD time series. A BOLD time series can be formed from the control and tag images through running average approaches that are analogous to the subtraction approaches used to form the perfusion time series. In general, the BOLD time series is formed by the convolution of the control and tag images with a lowpass filter (Liu & Wong, 2005). For example, the method analogous to surround subtraction would be a surround average consisting of the average of each image with the average of its two nearest neighbors. The BOLD time series is inherently flow-weighted because of the tagging process. In pulsed ASL experiments the flow weighting can be reduced by the application of a saturation pulse applied in the imaging plane either immediately prior to or immediately after the application of the tagging pulse (Liu & Wong, 2005; Wong et al., 1997). Applications of simultaneous BOLD and CBF estimates are described below in the section discussing the strengths of ASL.

Errors and limitations

Systematic measurement errors. The ASL difference signal ΔM is proportional to CBF but also has a complex dependence on a number of physiological parameters. Variations in these physiological parameters can cause systematic errors in the CBF measurements. *The goal of quantitative ASL methods is to minimize these errors.* The primary sources of errors are: (1) the *transit delay* Δt between the tagging region and the imaging slice; (2) the *temporal width* τ of the arterial bolus in PASL techniques; (3) the presence of intravascular tagged blood that has not yet perfused its target capillary bed; (4) the dependence of relaxation on the exchange of water between blood and tissue compartments; and (5) the clearance of water by outflow.

As shown in Figure 4, transit delays arise in spatial tagging methods because of the need to place the tagging slab in PASL or the tagging plane in CASL some distance (1–3 cm) from the imaging slice in order to minimize the inadvertent perturbation of spins in the imaging region by the tagging pulse. To allow all of the tagged blood to travel from the tagging region to the imaging region, the inversion time TI must satisfy the condition $TI > \Delta t + \tau$ where Δt is the transit delay and τ is the temporal width of the tagged bolus (Wong et al., 1998a). In contrast to CASL and PASL, transit delays are typically negligible in VS-ASL because

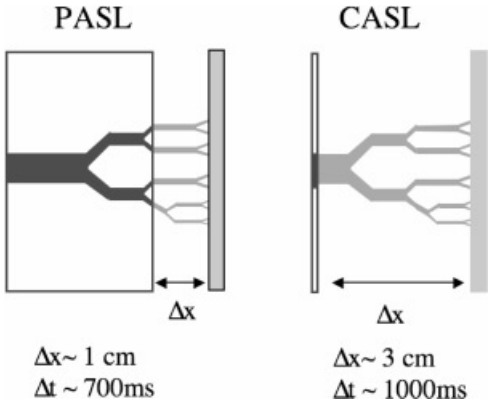

Fig. 4. Illustration of spatial gaps between the tagging (clear rectangles) and imaging (light gray) regions in pulsed ASL (PASL) and continuous ASL (CASL) and the associated transit delays.

the velocity-selective tagging process saturates arterial blood with velocities down to 1 to 2 cm/s, corresponding to vessels (roughly 50–100 μ arterioles) that are close to the capillary bed and within the imaging region. This insensitivity to transit delay makes VS-ASL a particularly attractive method for functional ASL studies of subjects, such as stroke patients, who may exhibit long transit delays.

In CASL methods the temporal bolus width τ is determined by the temporal duration (typically 1–3 seconds) of the continuous inversion pulse. However, in PASL methods the temporal width depends on the velocity of arterial blood in the tagging region, which typically increases with functional activation. To reduce the sensitivity to the temporal width, a spatial saturation pulse is applied to the tagging region at a time TI_1 after the inversion pulse. This is referred to as the QUIPSS II modification (Wong et al., 1998a). If $TI_1 < \tau$, then the temporal width of the bolus is TI_1, and the measured signal is proportional to the product of CBF and TI_1.

A related source of error is the presence of tagged blood in the arteries and arterioles that has entered the imaging slice but is destined to perfuse more distal slices. If the image is acquired before this blood has time to leave the imaging slice, the intravascular signal will contribute to the ASL difference signal and lead to an overestimate of CBF. Typically, this is not a problem when using pulse sequence parameters that also control for transit delays. In addition, flow-weighting gradients can be used to crush the intravascular signal at the cost of a reduction in the SNR of the desired difference signal (Ye et al., 1997).

Improper modeling of the exchange of water between blood and tissue components can lead to significant errors in CBF quantification, especially in tissues with low CBF, such as white matter (Parkes, 2005). For these cases, Parkes and Tofts (Parkes & Tofts, 2002) have shown that a simple two compartment model of exchange can be used to improve accuracy. Finally, errors due to the clearance of water by venous outflow are usually negligible given the inversion times used in most ASL experiments, but may need to be

considered in high flow conditions or when long inversion times are used (Parkes, 2005).

Temporal resolution. The temporal resolution of perfusion fMRI is inherently poorer than BOLD fMRI because of the necessity to form tag and control images and to allow time for blood to be delivered from the tagging region to the imaging slice. In a typical pulsed ASL experiment, a repetition time (TR) of 2 seconds or more is used, so that one tag and control image pair is acquired every 4 seconds. By comparison, the temporal resolution of BOLD fMRI is typically 1 to 2 seconds and can be as low as 100 ms for specialized applications (Dale & Buckner, 1997; Ogawa et al., 2000). The more coarse temporal resolution of ASL is offset somewhat by more modest temporal correlations in ASL perfusion methods than in BOLD (Aguirre et al., 2002). Methods for improving temporal resolution include turbo-ASL (Wong et al., 2000) and single-shot ASL (Duyn et al., 2001). Turbo-ASL shortens the imaging time by utilizing the image acquisition at a short delay (typically 100 ms) following the control to acquire the preceding tag signal, and *vice versa*. In single-shot ASL, background suppression is used to suppress static tissue, thus eliminating the need for a control image. While turbo-ASL and single-shot ASL can improve temporal resolution, the quantitation of the resultant ASL signals is more complicated than for more standard methods (Hernandez-Garcia et al., 2005).

Signal to noise and contrast to noise ratios. As discussed previously, the SNR of ASL methods is inherently low because the inflowing blood magnetization is typically only about 1 percent of the tissue. The low SNR combined with the poor temporal resolution of ASL results in a low contrast-to-noise ratio (CNR) for quantitative ASL fMRI experiments as compared to BOLD. Because of the low inherent SNR of ASL methods, noise reduction methods such as the physiological noise reduction method should be used wherever possible. Background suppression methods that attenuate the static tissue component also have the potential to reduce noise, but their application for simultaneous CBF/BOLD experiments is not straightforward (St. Lawrence et al., 2005). For functional mapping experiments where measurement of CBF is not required, non-quantitative versions of ASL, such as turbo-ASL (Wong et al., 2000) and close-tag CASL (Wong et al., 2001) can be used to improve the CNR. For example, the CNR of close-tag continuous CASL at 1.5 T has been shown to approach that of the BOLD signal for a finger-tapping experiment (Wong et al., 2001).

Although the signal to noise ratio of ASL perfusion is typically lower than for BOLD, the trade-off between detection sensitivity and efficiency in an ASL experiment is similar to the BOLD experiment (Liu et al., 2002). Design efficiency roughly reflects how much information each time series observation reveals about the underlying hemodynamic response. Considering the trade-off between detection power and efficiency can improve the design of ASL experiments, within the limits of signal to noise imposed by the mechanics of the experiment. Moreover, because ASL perfusion data show small and symmetrical temporal correlations down the time series, ASL data can be analyzed by permutation tests that might not be appropriate for BOLD time series data (Aguirre et al., 2005). When conventional assumptions of analysis of variance do not hold, permutation tests can yield more powerful statistical tests than conventional tests (Aguirre et al., 2005). The use of permutation statistics to analyze ASL data merits further study.

Spatial coverage. At present, most ASL fMRI studies use 2D multi-slice acquisition methods in which the data are acquired on a slice-by-slice basis. For CASL and PASL methods, the slices are typically acquired in an inferior-to-superior manner so that slices that are further from the tagging region are acquired at later times. The number of slices that can be acquired depends on the (a) acquisition time for each slice; (b) the time TR-TI that is available for slice acquisition; and (c) the need to acquire slices before the difference signal ΔM has decayed away because of the longitudinal relaxation of blood. Because of these considerations, ASL studies typically acquire a smaller number of slices (e.g. 3–15) than whole-brain BOLD studies (e.g. 30−40 slices), with thicker slices (e.g. 5–8 mm) than would be used in a BOLD study (e.g. 3 or 4 mm). Recently, ASL fMRI studies with single-shot 3D acquisitions have been demonstrated (Duhamel & Alsop, 2004; Fernandez-Seara et al., 2005). 3D acquisitions with refocusing pulse trains can reduce susceptibility-related artifacts, such as the severe signal dropouts that occur in the orbitofrontal cortex. In one study ASL perfusion was less sensitive to susceptibility effects associated with overt speech than was the BOLD response (Kemeny et al., 2005). Three-dimensional methods are also well-suited to the use of background suppression methods and are a natural match for the non-spatial tagging scheme used in VS-ASL. However, 3D methods are not well suited for simultaneous measurements of CBF and BOLD.

Strengths

Quantitative assessment of neural activity. Because it can provide a quantitative measure of a fundamental physiological quantity (CBF), ASL has the potential to better reflect neural activity as compared to BOLD, which is a complex function of a number of physiological variables, especially oxygen utilization, cerebral blood flow, and cerebral blood volume. For example, the findings of one ASL study suggest that the relation between CBF changes and neural activity may be more linear than the relation between BOLD and neural activity (Miller et al., 2001). Several studies have shown that ASL measures can exhibit decreased inter-subject and inter-session variability as compared to BOLD, possibly reflecting a more direct link between CBF and neural activity (Aguirre et al., 2002; Tjandra et al., 2005; Wang et al., 2003).

When combined with BOLD measures, ASL measures of CBF can be used to derive estimates of functional changes in the cerebral metabolic rate of oxygen ($CMRO_2$), which has been shown in animal studies to be correlated with functional changes in neuronal activity (Hyder, 2004). In human fMRI studies, the use of simultaneous measurements of CBF and BOLD responses to a hypercapnic stimulus (administered carbon dioxide) can provide information that is then used to calibrate the BOLD response and estimate functional changes in $CMRO_2$ (Davis et al., 1998). This approach has been used to demonstrate a linear coupling in the visual cortex between functional changes in CBF and $CMRO_2$ (Hoge et al., 1999).

Simultaneous measures of CBF and BOLD with ASL are also useful for understanding the mechanisms underlying the BOLD response. For example, Obata et al. (2004) found that the BOLD responses in the supplementary motor area exhibited pronounced transients at stimulus onset and cessation that were not observed in the CBF data, suggesting that the BOLD transients primarily reflected vascular as opposed to neural effects. Similarly, ASL measurements have been used to examine whether post-stimulus undershoots in the BOLD signal are caused primarily by a slow return to baseline in cerebral blood volume or to a prolonged elevation of $CMRO_2$ (Buxton et al., 1998b; Lu et al., 2004).

Insensitivity to low-frequency noise. Low frequency drifts are present in most fMRI time series data and tend to reduce the statistical power of BOLD experiments. As discussed in a previous section, perfusion time series are formed from the filtered subtraction of control and tag images. This subtraction process greatly attenuates the low frequency drifts and can make ASL more sensitive than BOLD for experimental paradigms with long periods (Aguirre et al., 2002). For example, one study has shown that the sensitivity of ASL is greater than that of BOLD when the alternating period between task and control is greater than a few minutes (Wang et al., 2003). In a recent study assessing the effects of psychological stress on CBF, the insensitivity of ASL to low frequency drifts enabled the investigators to demonstrate an increase in CBF that persisted for at least eight minutes after the completion of a stressful task (Wang et al., 2005).

Spatial localization. Because perfusion methods directly measures the amount of arterial blood that has been delivered to the capillary bed, the functional CBF signal may be more localized to the sites of neuronal activation than the BOLD signal. With quantitative ASL methods, the measured CBF signal is primarily from small arterioles, capillaries, and brain tissue. There is relatively little signal in the arteries because the inversion delays are chosen to allow enough time for the blood to flow to the target tissue. In addition, there is relatively little outflow of the tagged blood into the venous circulation, because (a) the inversion delays are on the order of the T_1 of blood, which is much less than the capillary transit time, and (b) there is rapid exchange of water between the vascular and tissue compartments. By contrast, the BOLD signal derives primarily from veins and their surrounding tissues. Evidence in support of improved localization with ASL comes from a study which found that the average T_1 of voxels demonstrating a large ASL signal was close to that of gray matter, whereas the average T_1 of voxels demonstrating large BOLD signal was intermediate between those of gray matter, blood, and CSF (Luh et al., 2000). Similarly, in a study of visual orientation columns in the cat brain, it was found that the ASL signal provided a more convincing functional map of these very high resolution structures than the BOLD signal (Kim & Duong, 2002).

Table 1 presents a summary of the strengths and weaknesses of using ASL signals to measure neuronal activity during behavioral challenge tasks.

Table 1. Comparison of arterial spin labeling and blood oxygenation level dependent imaging methods of measuring functional brain activity

Advantages of ASL Compared with BOLD	Disadvantages of ASL Compared with BOLD
The ASL perfusion signal measures a well defined physiological quantity that can exhibit decreased inter-subject and inter-session variability as compared to BOLD.	The signal to noise ratio of the ASL response is typically less than half that of the BOLD response
ASL processing methods make use of a differencing approach that minimizes the effects of low frequency drifts and makes ASL ideal for experiments with long stimulus durations	The temporal resolution of ASL methods is poorer than that of typical BOLD acquisitions because of the need to acquire two sets of images (tag and control) and the need to wait for blood to flow into the imaging region.
ASL methods can be used with imaging methods, such as spin-echo readouts, that reduce susceptibility-related signal losses.	The maximum number of slices that can be acquired with ASL is usually less than that of BOLD due to the need to acquire data before the tagged blood signal has fully relaxed.
The ASL perfusion signal is well localized to the capillary beds	

SUMMARY

Imaging sequences based on BOLD contrast are currently the predominant method for functional magnetic resonance imaging (fMRI) of the brain. BOLD weighted sequences offer high contrast-to-noise ratio and good temporal resolution. However, the BOLD signal reflects the magnetic susceptibility effects of total deoxyhemoglobin ($dHBO_2$) and is thus a complex function of cerebral blood flow (CBF), the cerebral rate of oxygen metabolism ($CMRO_2$), cerebral blood volume (CBV), and magnetic field strength. The interpretation of changes in the BOLD signal can be complicated by variations in any of these physiological quantities caused by age, disease, or the presence of vasoactive agents (D'Esposito et al., 2003). Perfusion fMRI, based on arterial spin labeling (ASL) methods, offers a useful complement to BOLD fMRI. It can provide quantitative measures of both baseline and functional changes in CBF that can aid in the interpretation of the BOLD signal change. Changes in CBF are believed to be more directly linked to neuronal activity than BOLD, so that perfusion fMRI also has the potential to offer more accurate measures of the spatial location and magnitude of neural function. Perfusion fMRI also has practical advantages, including an inherent insensitivity to low-frequency fluctuations commonly observed in fMRI experiments and the ability to take advantage of imaging sequences (e.g., spin-echo) that are insensitive to susceptibility induced off-resonance effects, which cause signal drop-out. As ASL methods have become increasingly sophisticated, they have become increasingly useful in studies of brain-behavior relationships in health and disease.

ACKNOWLEDGMENTS

Preparation of this paper was supported by the VISN 22 Mental Illness Research Education and Clinical Center, a Biomedical Engineering Research Grant from the Whitaker Foundation, and by NIH grants #1 U24 RR021992 to the Function Biomedical Informatics Research Network (FBIRN, http://www.nbirn.net), 1 RO1 NS051661 to the first author, and 1 R01 NS367220 to Richard Buxton. The authors thank Wen-Ming Luh, Joanna Perthen, Khaled Restom, and Eric Wong for their contributions to the figures and text. The figures presented here were previously published in the syllabus for an educational talk titled Perfusion-Based fMRI presented at the 14th Scientific Meeting of the International Society for Magnetic Resonance in Medicine (Seattle 2006).

REFERENCES

Aguirre, G.K., Detre, J.A., & Wang, J. (2005). Perfusion fMRI for functional neuroimaging. *International Review of Neurobiology*, *66*, 213–236.

Aguirre, G.K., Detre, J.A., Zarahn, E., & Alsop, D.C. (2002). Experimental design and the relative sensitivity of BOLD and perfusion fMRI. *NeuroImage*, *15*, 488–500.

Alsop, D.C. (2005). Perfusion imaging of the brain: Contribution to clinical MRI. In R.R. Edelman, J.R. Hesselink, M.B. Zlatkin, & J.V. Cures III (Eds.), *Clinical magnetic resonance imaging* (3rd ed.), Vol. 1 (pp. 333–357). Philadelphia: Saunders Elsevier.

Buxton, R.B. (2002). *Introduction to functional Magnetic Resonance Imaging*. Cambridge, UK: Cambridge University Press.

Buxton, R.B., Frank, L.R., Wong, E.C., Siewert, B., Warach, S., & Edelman, R.R. (1998a). A general kinetic model for quantitative perfusion imaging with arterial spin labeling. *Magnetic Resonance in Medicine*, *40*, 383–396.

Buxton, R.B., Wong, E.C., & Frank, L.R. (1998b). Dynamics of blood flow and oxygenation changes during brain activation: The balloon model. *Magnetic Resonance in Medicine*, *39*, 855–864.

Calamante, F., Thomas, D.L., Pell, G.S., Wiersma, J., & Turner, R. (1999). Measuring cerebral blood flow using magnetic resonance imaging techniques. *Journal of Cerebral Blood Flow and Metabolism*, *19*, 701–735.

Dale, A.M. & Buckner, R.L. (1997). Selective averaging of rapidly presented individual trials using fMRI. *Human Brain Mapping*, *5*, 329–340.

Davis, T.L., Kwong, K.K., Weisskoff, R.M., & Rosen, B.R. (1998). Calibrated functional MRI: Mapping the dynamics of oxidative metabolism. *Proceedings of the National Academy of Science USA*, *95*, 1834–1839.

D'Esposito, M., Deouell, L.Y., & Gazzaley, A. (2003). Alterations in the BOLD fMRI signal with ageing and disease: A challenge for neuroimaging. *Nature Reviews Neuroscience*, *4*, 863–872.

Detre, J.A., Leigh, J.S., Williams, D.S., & Koretsky, A.P. (1992). Perfusion imaging. *Magnetic Resonance in Medicine*, *23*, 37–45.

Duhamel, G. & Alsop, D.C. (2004). *Single-shot susceptibility insensitive whole brain 3D fMRI with ASL.* Paper presented at the 12th ISMRM Scientific Meeting, Kyoto, Japan.

Duyn, J.H., Tan, C.X., van Gelderen, P., & Yongbi, M.N. (2001). High-sensitivity single-shot perfusion-weighted fMRI. *Magnetic Resonance in Medicine*, *46*, 88–94.

Edelman, R.R., Siewert, B., Darby, D.G., Thangaraj, V., Nobre, A.C., Mesulam, M.M., & Warach, S. (1994). Qualitative mapping of cerebral blood flow and functional localization with echo-planar MR imaging and signal targeting with alternating radio frequency. *Radiology*, *192*, 513–520.

Fernandez-Seara, M.A., Wang, J., Wang, Z., Rao, H., Guenther, M., Feinberg, D.A., & Detre, J.A. (2005). *Continuous arterial spin labeling perfusion measurements using single shot 3D GRASE at 3T*. Paper presented at the 13th ISMRM Scientific Meeting, Miami Beach, Florida, USA.

Garcia, D.M., Bazelaire, C.D., & Alsop, D. (2005). *Pseudo-continuous flow drive adiabatic inversion for arterial spin labeling*. Paper presented at the 13th ISMRM Scientific Meeting, Miami Beach, Florida, USA.

Guyton, A.C. (1977). *Basic human physiology: Normal function and mechanisms of disease* (2nd ed.). Philadelphia: W. B. Saunders Company.

Hernandez-Garcia, L., Lee, G.R., Vazquez, A.L., Yip, C.Y., & Noll, D.C. (2005). Quantification of perfusion fMRI using a numerical model of arterial spin labeling that accounts for dynamic transit time effects. *Magnetic Resonance in Medicine*, *54*, 955–964.

Hoge, R.D., Atkinson, J., Gill, B., Crelier, G.R., Marrett, S., & Pike, G.B. (1999). Linear coupling between cerebral blood flow and oxygen consumption in activated human cortex. *Proceedings of the National Academy of Science USA*, *96*, 9403–9408.

Hyder, F. (2004). Neuroimaging with calibrated FMRI. *Stroke*, *35* (Suppl. 1), 2635–2641.

Kim, S.-G. & Duong, T.Q. (2002). Mapping cortical columnar structures using fMRI. *Physiology & Behavior*, *77*, 641–644.

Kim, S.-G. & Tsekos, N.V. (1997). Perfusion imaging by a flow-sensitive alternating inversion recovery (FAIR) technique: Application to functional brain imaging. *Magnetic Resonance in Medicine*, *37*, 425–435.

Kwong, K.K., Chesler, D.A., Weisskoff, R.M., Donahue, K.M., Davis, T.L., Ostergaard, L., Campbell, T.A., & Rosen, B.R. (1995). MR perfusion studies with T1-weighted echo planar imaging. *Magnetic Resonance in Medicine*, *34*, 878–87.

Liu, T.T. & Wong, E.C. (2005). A signal processing model for arterial spin labeling functional MRI. *NeuroImage*, *24*, 207–215.

Liu, T.T., Wong, E.C., Frank, L.R., & Buxton, R.B. (2002). Analysis and design of perfusion-based event-related fMRI experiments. *NeuroImage*, *16*, 269–282.

Lu, H., Golay, X., Pekar, J.J., & Van Zijl, P.C. (2004). Sustained poststimulus elevation in cerebral oxygen utilization after vascular recovery. *Journal of Cerebral Blood Flow and Metabolism*, *24*, 764–770.

Luh, W.M., Wong, E.C., Bandettini, P.A., Ward, B.D., & Hyde, J.S. (2000). Comparison of simultaneously measured perfusion and BOLD signal increases during brain activation with T(1)-based tissue identification. *Magnetic Resonance in Medicine*, *44*, 137–143.

Kemeny, S., Ye, F.Q., Birn, R., & Braun, A.R. (2005). Comparison of continuous overt speech fMRI using BOLD and arterial spin labeling. *Human Brain Mapping*, *24*, 173–183.

Meier, P. & Zierler, K.L. (1954). On the theory of the indicator-dilution method for measurement of blood flow and volume. *Journal of Applied Physiology*, *6*, 731–744.

Miller, K.L., Luh, W.M., Liu, T.T., Martinez, A., Obata, T., Wong, E.C., Frank, L.R., & Buxton, R.B. (2001). Nonlinear temporal dynamics of the cerebral blood flow response. *Human Brain Mapping*, *13*, 1–12.

Mumford, J.A., Hernandez-Garcia, L., Lee, G.R., & Nichols, T.A. (2006). Estimation efficiency and statistical power in arterial spin labeling fMRI. *NeuroImage*, *33*, 103–114.

Obata, T., Liu, T.T., Miller, K.L., Luh, W.M., Wong, E.C., Frank, L.R., & Buxton, R.B. (2004). Discrepancies between BOLD and flow dynamics in primary and supplementary motor areas: Application of the balloon model to the interpretation of BOLD transients. *NeuroImage*, *21*, 144–153.

Ogawa, S., Lee, T.-M., Stepnoski, R., Chen, W., Zhu, X.-H., & Ugurbil, K. (2000). An approach to probe some neural systems interaction by functional MRI at neural time scale down to milliseconds. *Proceedings of the National Academy of Science. USA*, *97*, 11026–11031.

Parkes, L.M. (2005). Quantification of cerebral perfusion using arterial spin labeling: Two-compartment models. *Journal of Magnetic Resonance Imaging*, *22*, 732–736.

Parkes, LM. & Tofts, P.S. (2002). Improved accuracy of human cerebral blood perfusion measurements using arterial spin labeling: Accounting for capillary water permeability. *Magnetic Resonance in Medicine*, *48*, 27–41.

Restom, K., Behzadi, Y., & Liu, T.T. (2006). Physiological noise reduction for arterial spin labeling functional MRI. *Neuro Image*, *31*, 1104–1115.

Roy, C.S. & Sherrington, C.S. (1890). On the regulation of the blood-supply of the brain. *The Journal of Physiology*, *11*, 85–108.

St. Lawrence, K.S., Frank, J.A., Bandettini, P.A., & Ye, F.Q. (2005). Noise reduction in multi-slice arterial spin tagging imaging. *Magnetic Resonance in Medicine*, *53*, 735–738.

Tjandra, T., Brooks, J.C., Figueiredo, P., Wise, R., Matthews, P.M., & Tracey, I. (2005). Quantitative assessment of the reproducibility of functional activation measured with BOLD and MR perfusion imaging: Implications for clinical trial design. *NeuroImage*, *27*, 393–401.

Wang, J., Aguirre, G.K., Kimberg, D.Y., Roc, A.C., Li, L., & Detre, J.A. (2003). Arterial spin labeling perfusion fMRI with very low task frequency. *Magnetic Resonance in Medicine*, *49*, 796–802.

Wang, J., Rao, H., Wetmore, G.S., Furlan, P.M., Korczykowski, M., Dinges, D.F., & Detre, J.A. (2005). Perfusion functional MRI reveals cerebral blood flow pattern under psychological stress. *Proceedings of the National Academy of Sciences, USA*, *102*, 17804–17809.

Warner, D.S., Kassell, N.F., & Boarini, D.J. (1987). Microsphere cerebral blood flow determination. In J.H. Wood (Ed.), *Cerebral blood flow: Physiologic and clinical aspects* (pp. 288–298). New York: McGraw-Hill Company.

Williams, D.S., Detre, J.A., Leigh, J.S., & Koretsky, A.P. (1992). Magnetic resonance imaging of perfusion using spin inversion of arterial water. *Proceedings of the National Academy of Science USA*, *89*, 212–216.

Wintermark, M., Sesay, M., Barbier, E., Borbely, K., Dillon, W.P., Eastwood, J.D., Glenn, T.C., Grandin, C.B., Pedraza, S., Soustiel, J.F., Nariai, T., Zaharchuk, G., Caille, J.M., Dousset, V., & Yonas, H. (2005). Comparative overview of brain perfusion imaging techniques. *Journal of Neuroradiology*, *32*, 294–314.

Wong, E.C., Buxton, R.B., & Frank, L.R. (1997). Implementation of quantitative perfusion imaging techniques for functional brain mapping using pulsed arterial spin labeling. *NMR in Biomedicine*, *10*, 237–249.

Wong, E.C., Buxton, R.B., & Frank, L.R. (1998a). Quantitative imaging of perfusion using a single subtraction (QUIPSS and QUIPSS II). *Magnetic Resonance in Medicine*, *39*, 702–708.

Wong, E.C., Buxton, R.B., & Frank, L.R. (1998b). A theoretical and experimental comparison of continuous and pulsed arterial spin labeling techniques for quantitative perfusion imaging. *Magnetic Resonance in Medicine*, *40*, 348–355.

Wong, E.C., Cronin, M., Wu, W.C., Inglis, B., Frank, L.R., & Liu, T.T. (2006). Velocity-selective arterial spin labeling. *Magnetic Resonance in Medicine*, *55*, 1334–1341.

Wong, E.C., Liu, T.T., Frank, L.R., & Buxton, R.B. (2001). *Close tag*, *short TR continuous ASL for functional brain mapping: High temporal resolution ASL with a BOLD sized signal at 1.5T*. Paper presented at the Ninth Meeting, International Society for Magnetic Resonance in Medicine, Glasgow, Scotland, UK.

Wong, E.C., Luh, W.M., & Liu, T.T. (2000). Turbo ASL: Arterial spin labeling with higher SNR and temporal resolution. *Magnetic Resonance in Medicine*, *44*, 511–515.

Woolrich, M.W., Chiarelli, P., Gallichan, D., Perthen, J., & Liu, T.T. (2006). Inferring blood volume, blood flow, and blood oxygenation changes from functional ASL data. *Magnetic Resonance in Medicine*, *56*, 891–906.

Ye, F.Q., Matay, V.S., Jezzard, P., Frank, J.A., Weinberger, D.R., & McLaughlin, A.C. (1997). Correction for vascular artifacts in cerebral blood flow values measured by using arterial spin tagging techniques. *Magnetic Resonance in Medicine*, *37*, 226–235.